Suspension Bridges

Abstract

We study suspension bridges. We start with a simple curved deck bridge model on two dimensions and derive the dynamic equations. We study the oscillations of the bridge by considering separate dimensions and both dimensions. We find the normal modes and solve the dynamic equations. We then consider the oscillations of a load applied to the model. We investigate the relation of our model to the collapse of a bridge and make further implications.

1 Introduction

Suspension bridges are significant infrastructures to humans nowadays for transportation. Smaller bridges like pedestrian bridges are also widely used nowadays. Due to the great importance of these bridges have on our daily lives, accidents related to them may cause unimaginable results on our lives, however minor the accidents may seem. In 1940, the Tacoma Narrows Bridge collapsed [1], which aroused great attention amongst many scientists and engineers to investigate its cause. Therefore, we want to delve into the structure of a suspension bridge and consider the factors that make it oscillate, which include the bridge's normal mode of oscillation, wind excitation and load attachment. By finding the cause we can improve the building techniques and take measures against the collapse of the suspension bridge, potentially reducing the number of human injuries or deaths.

In this essay, we will focus on a curved deck suspension bridge model, and also briefly look into the feasibility of the application of our model to flat deck bridges. We start by delving into the dynamic equations of a bridge from two dimensions. We will first consider two approximations, simplifying the general equations by restricting ourselves to the vertical or horizontal components. By applying several mathematical and computational techniques, including expressing the equations in matrix form, Taylor expansion, and solving ordinary differential equations, we can obtain the normal mode profiles and frequencies of the pedestrian bridge. We then repeat but consider the full equation on both vertical and horizontal displacements and make comparisons.

We will then move on to study the dynamic equations with a load on the bridge. We will consider the load approximating a person jumping at different frequencies and different positions and compare the results of the maximum vertical amplitudes generated by the bridge to make further implications from physics and engineering point of view.

Before we delve into our bridge model, let us first introduce the structure of a suspension bridge.

2 Structure and types of suspension bridges

A suspension bridge usually refers to the type of bridge in which the deck is hung below suspension cables on vertical suspenders.[2] This is a flat deck bridge, in which the deck segments are suspended below the cable.

In this essay, We will mainly focus on modelling the other type of suspension bridge, which is a curved deck bridge where the deck is on the suspension cable. They can serve as pedestrian bridges. The deck segments are attached to the bridge through nodes. There are two parallel cables on each side of the bridge, with two nodes on each side of each deck segment but we will only consider our model on 2 dimensions, i.e. one side of the bridge.

3 Dynamic equations

To know about the dynamics behind the structure of the bridge, we may want to study its force diagram:

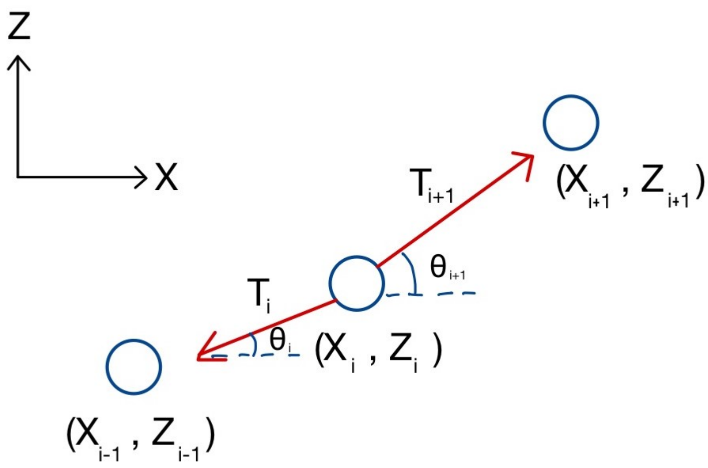

Figure 1: Force diagram of 3 of the nodes of a bridge

We label T_i the tension in the suspension cable section between node $i-1$ and node i. We also denote θ_i the angle between the two nodes from the positive horizontal axis. Then by balancing the horizontal and vertical forces, we have :

$$\begin{aligned} T_i\cos(\theta_i) - T_{i+1}\cos(\theta_{i+1}) &= 0 \\ T_{i+1}\sin(\theta_{i+1}) - T_i\sin(\theta_i) &= Mg \end{aligned} \tag{1}$$

Let $T = T_i\cos(\theta_i)$, which is a constant. As derived from (1), we have

$$T(\tan(\theta_{i+1}) - \tan(\theta_i)) = Mg \tag{2}$$

At the rest configuration of the bridge, we then have

$$\begin{aligned} \theta_{\frac{N}{2}} &= 0 \\ \tan(\theta_i) &= \tan(\theta_{i+1}) - \frac{Mg}{T}, \qquad i < \frac{N}{2}, \\ \tan(\theta_i) &= \tan(\theta_{i-1}) + \frac{Mg}{T}, \qquad i > \frac{N}{2} \end{aligned} \tag{3}$$

where N is the number of nodes which we assume is even, and θ_i is negative when $i < \frac{N}{2}$.

Now, we want to set a condition on the suspension bridge such that the bridge aligns in the way with an appropriate curvature. We first make a proposition as follows.

Let $P(i)$ be the proposition that **Q1**

$$\tan(\theta_{i+1}) = \left(i - \frac{N}{2}\right)\frac{Mg}{T} \tag{4}$$

where i is any integer from $\frac{N}{2}$ to $N-1$ inclusively.

First, let us consider the base case.
When $i = \frac{N}{2}$, from (3), we have

$$\begin{aligned}\tan(\theta_{\frac{N}{2}+1}) &= \tan(\theta_{\frac{N}{2}}) + \frac{Mg}{T} \\ \tan(\theta_{\frac{N}{2}+1}) &= \frac{Mg}{T}\end{aligned} \tag{5}$$

From (3), we also have

$$\begin{aligned}\tan(\theta_{\frac{N}{2}+2}) &= \tan(\theta_{\frac{N}{2}+1}) + \frac{Mg}{T} \\ \tan(\theta_{\frac{N}{2}+2}) &= \frac{2Mg}{T}\end{aligned} \tag{6}$$

Hence, $P\left(\frac{N}{2}\right)$ is true.

Now, assume $P(k)$ is true for some integers k.
When $i = k + 1$,

$$\begin{aligned}\tan(\theta_{k+1}) &= \tan(\theta_k) + \frac{Mg}{T} \\ &= \left(k - \frac{N}{2}\right)\frac{Mg}{T} + \frac{Mg}{T} \\ &= \left(k + 1 - \frac{N}{2}\right)\frac{Mg}{T}\end{aligned} \tag{7}$$

Hence, $P(k + 1)$ is true, which implies the proposition (4) is true for all integers i from $\frac{N}{2}$ to $N - 1$ inclusively.
We then have

$$\begin{aligned}\tan(\theta_{N-1}) &= \left(N - 1 - \frac{N}{2}\right)\frac{Mg}{T} \\ \tan(\theta_{N-1}) &= \frac{N-2}{2}\frac{Mg}{T} \\ \frac{Mg}{T} &= \frac{2}{N-2}\tan(\theta_{N-1})\end{aligned} \tag{8}$$

We let $\theta_{tower} = \theta_{N-1}$. Then, we have

$$\frac{Mg}{T} = \frac{2}{N-2}\tan(\theta_{tower}). \tag{9}$$

Using (9), we can set $\theta_{tower} = \frac{\pi}{6}$ by adjusting the tension in the suspension cable.
In the scaling limit, as the number of nodes increase and the bridge is continuous, We can then mathematically deduce that the bridge profile can be represented by a parabola with equation

$$Z(x) = \frac{Mg}{2TL}x^2. \tag{10}$$

Denote K_{sc} the spring constant of the bridge cables. We want to study the bridge oscillation around the rest configuration of the bridge for each node. We first denote X_i and Z_i as the horizontal and vertical relative displacements of each node i.
Consider the equations

$$\begin{aligned}M\frac{d^2Z_i}{dt^2} &= F_{z,i} \\ M\frac{d^2X_i}{dt^2} &= F_{x,i}\end{aligned} \tag{11}$$

where

$$\begin{aligned} F_{z,i} &= K_{sc}[(Z_{i-1}-Z_i)\sin^2(\theta_i)+(Z_{i+1}-Z_i)\sin^2(\theta_{i+1})+ \\ &\quad +(X_{i-1}-X_i)\sin(\theta_i)\cos(\theta_i)+(X_{i+1}-X_i)\sin(\theta_{i+1})\cos(\theta_{i+1})] \end{aligned} \tag{12}$$

and

$$\begin{aligned} F_{x,i} &= K_{sc}[(X_{i-1}-X_i)\cos^2(\theta_i)+(X_{i+1}-X_i)\cos^2(\theta_{i+1})+ \\ &\quad +(Z_{i-1}-Z_i)\sin(\theta_i)\cos(\theta_i)+(Z_{i+1}-Z_i)\sin(\theta_{i+1})\cos(\theta_{i+1})]. \end{aligned} \tag{13}$$

For small θ_i, the sine terms approaches zero and hence we can ignore these terms and simplify the second equation to:

$$M\frac{d^2X_i}{dt^2}=K_{sc}[(X_{i-1}-X_i)\cos^2(\theta_i)+(X_{i+1}-X_i)\cos^2(\theta_{i+1}) \tag{14}$$

which considers only the horizontal displacement of the bridge. We will denote the model as model X.

We can also restrict the other equation to only the vertical displacements of the bridge. Since smaller forces give rise to greater displacements by inertia, we can simplify the first equation to:

$$M\frac{d^2Z_i}{dt^2}=K_{sc}[(Z_{i-1}-Z_i)\sin^2(\theta_i)+(Z_{i+1}-Z_i)\sin^2(\theta_{i+1}) \tag{15}$$

which we denote the model as model Z.

4 The Suspension Bridge Model

When a suspension bridge oscillates, there are some natural patterns and frequencies that they tend to oscillate and maintain at, where every component move in the same frequency. They are called the normal modes of the bridge.

In order to solve (14), we first assume the solution to be in the form :

$$X_i(t)=Y_i\sin(\omega t). \tag{16}$$

By substitution in (14), we have

$$-\omega^2Y_i=\frac{K_{sc}}{M}[(Y_{i-1}-Y_i)\cos^2(\theta_i)+(Y_{i+1}-Y_i)\cos^2(\theta_{i+1}) \tag{17}$$

which we can rewrite it as:

$$AY=-\omega^2Y \tag{18}$$

where

$$A_{i,j}=\frac{K_{sc}}{M}\left(-\delta_{i,j}(\cos^2(\theta_i)+\cos^2(\theta_{i+1}))+\delta_{i+1,j}\cos^2(\theta_{i+1})+\delta_{i-1,j}\cos^2(\theta_i)\right). \tag{19}$$

We denote $\delta_{i,j}$ the Kronecker symbol which equals to 1 if $i=j$ and 0 if $i\neq j$. When we solve the equation using (15), we will still use (18) but we will change the matrix A to:

$$A_{i,j}=\frac{K_{sc}}{M}\left(-\delta_{i,j}(\sin^2(\theta_i)+\sin^2(\theta_{i+1}))+\delta_{i+1,j}\sin^2(\theta_{i+1})+\delta_{i-1,j}\sin^2(\theta_i)\right). \tag{20}$$

We can modify (17) to solve it in the limit that the tension in the cable gets extremely large and the thetas get very small. Then (17) becomes

$$-\omega^2Y_i=\frac{K_{sc}}{M}(Y_{i-1}-2Y_i+Y_{i+1}). \tag{21}$$

In the continuum limit, since the Y_i are continuous we can take $Y_i = Y(x)$ with

$$Y_i = Y(i * L) \tag{22}$$

where we denote L the length of each segment.

Q2

By Taylor expansion of Y_{i+1} about Y_i,

$$\begin{aligned} Y_{i+1} &= Y((i+1)L) \\ &= Y(iL+L) \\ &= Y(iL) + LY'(iL) + \frac{L^2}{2}Y''(iL) + O(L^3) \end{aligned} \tag{23}$$

By Taylor expansion of Y_{i-1} about Y_i,

$$\begin{aligned} Y_{i-1} &= Y((i-1)L) \\ &= Y(iL-L) \\ &= Y(iL) - LY'(iL) + \frac{L^2}{2}Y''(iL) - O(L^3) \end{aligned} \tag{24}$$

Hence, by substituting the two expansions,

$$\begin{aligned} & Y_{i-1} - 2Y_i + Y_{i+1} \\ = \;& Y(iL) - 2Y(iL) + Y(iL) - LY'(iL) + LY'(iL) + \frac{L^2}{2}Y''(iL) + \frac{L^2}{2}Y''(iL) + O(L^3) - O(L^3) \\ = \;& L^2(Y''(iL)) \end{aligned} \tag{25}$$

Thus, we have

$$-\omega^2 Y(iL) = \frac{L^2 K_{sc}}{M} Y''(iL) \tag{26}$$

In the continuum limit, by taking $Y_i = Y(x)$, then we get:

$$-\omega^2 Y(x) = \frac{L^2 K_{sc}}{M}\frac{d^2Y(x)}{x^2}. \tag{27}$$

Now that we have obtained (27), it looks way easier to solve by hand as it is just an ordinary second-order differential equation. Let us try to find the solutions of (27).

Q3

To solve a second order ordinary differential equation, we solve the quadratic equation:

$$\frac{L^2 K_{sc}}{M}\lambda^2 + \omega^2 = 0 \tag{28}$$

$$\lambda = \pm\sqrt{\frac{M\omega^2}{L^2 K_{sc}}}i \tag{29}$$

Hence, we can consider the solution $Y(x)$
to be the form $Y = A\cos\left(\sqrt{\frac{M\omega^2}{L^2K_{sc}}}x\right) + B\sin\left(\sqrt{\frac{M\omega^2}{L^2K_{sc}}}x\right)$, where A and B are constants. Upon substitutions of the initial conditions, we have the two equations

$$\begin{aligned} Y(0) &= A = 0 \\ Y(D) &= B\sin\left(\sqrt{\frac{M\omega^2}{L^2K_{sc}}}D\right) = 0 \end{aligned} \tag{30}$$

where D is the bridge length. This implies that

$$B = 0 \quad \text{or} \quad \sqrt{\frac{M\omega^2}{L^2 K_{sc}}} D = \pi k \tag{31}$$

where k is an integer.
Finally, we deduce that

$$Y(x) = 0 \quad \text{(rejected)} \quad \text{or} \quad Y(x) = B\sin\left(\frac{\pi k}{D} x\right) \tag{32}$$

where k is an integer and B is a real constant
Hence,

$$\omega = \frac{\pi k L}{D}\sqrt{\frac{K_{sc}}{M}} \tag{33}$$

where k is an integer.

In addition, we may also compute the full dynamics equations (11) using solutions of the form: $X_i(t) = x_i\sin(\omega t)$ and $Z_i(t) = z_i\sin(\omega t)$. By substitution, we get the two equations:

$$\begin{aligned}
-\omega^2 z_i &= \frac{K_{sc}}{M}[(z_{i-1} - z_i)\sin^2(\theta_i) + (z_{i+1} - z_i)\sin^2(\theta_{i+1}) + \\
&\quad +(x_{i-1} - x_i)\sin(\theta_i)\cos(\theta_i) + (x_{i+1} - x_i)\sin(\theta_{i+1})\cos(\theta_{i+1})] \\
-\omega^2 x_i &= \frac{K_{sc}}{M}[(x_{i-1} - x_i)\cos^2(\theta_i) + (x_{i+1} - x_i)\cos^2(\theta_{i+1}) + \\
&\quad +(z_{i-1} - z_i)\sin(\theta_i)\cos(\theta_i) + (z_{i+1} - z_i)\sin(\theta_{i+1})\cos(\theta_{i+1})]
\end{aligned} \tag{34}$$

To avoid null eigenvalues generated that correspond to the free movements of the bridge nodes, we also need to add to the vertical force the following expression to ensure rigidity of our suspension cable:

$$K_{bend}\left(\frac{Z_{i-1} + Z_{i+1}}{2} - Z_i\right) \tag{35}$$

where K_{bend} is the bending coefficient.

We can rewrite (34) in the matrix form (18) with the first N elements of Y corresponding to X, and the remaining to Z :

$$\begin{aligned}
Y_i &= x_i, \\
Y_{N+i} &= z_i, \\
A_{i,j} &= \frac{K_{sc}}{M}\left(-\delta_{i,j}(\cos^2(\theta_i) + \cos^2(\theta_{i+1})) + \delta_{i+1,j}\cos^2(\theta_{i+1}) + \delta_{i-1,j}\cos^2(\theta_i)\right) \\
A_{N+i,N+j} &= \frac{K_{sc}}{M}\left(-\delta_{i,j}(\sin^2(\theta_i) + \sin^2(\theta_{i+1})) + \delta_{i+1,j}\sin^2(\theta_{i+1}) + \delta_{i-1,j}\sin^2(\theta_i)\right) \\
&\quad + \frac{K_{bend}}{M}\left(-\delta_{i,j} + \frac{1}{2}(\delta_{i+1,j} + \delta_{i-1,j})\right) \\
A_{i,N+j} = A_{N+i,j} &= \frac{K_{sc}}{M}(-\delta_{i,j}(\sin(\theta_i)\cos(\theta_i) + \sin(\theta_{i+1})\cos(\theta_{i+1})) \\
&\quad +\delta_{i+1,j}\sin(\theta_{i+1})\cos(\theta_{i+1}) + \delta_{i-1,j}\sin(\theta_i)\cos(\theta_i)
\end{aligned} \tag{36}$$

where $i, j \in [0, N)$.

With these equations solved, we can now compute and generate, using Python programs, the normal mode profiles and frequencies of our suspension bridge.

In our model, we consider a pedestrian bridge of 19 cable sections with the properties as follows:
Length of each section = 1m,
Weight of each section m = 30kg, thus M =15kg,
$K_{sc} = 5 \times 10^7 N/\text{m}$,
Angle at the tower $\theta_{tower} = 30°$.

Next, let us also compute some basic quantities about the bridge we want to model. Denote $\mathcal{L}$ the distance between the bases of the 2 bridge and h as the depth of the bridge.

Q5

$$\begin{aligned} \text{Distance } \mathcal{L} &= L(\cos\theta_1 + \cos\theta_2 + \cos\theta_3 + ... + \cos\theta_{N-1}) \\ &= 17.9877 \text{ m} \quad (\text{to 4 d.p.}) \end{aligned} \tag{37}$$

$$\begin{aligned} \text{Depth } h &= L(\sin\theta_{N/2} + \cos\theta_{N/2+1} + \sin\theta_{N/2+2} + ... + \sin\theta_{N-1}) \\ &= 2.6597 \text{ m} \quad (\text{to 4 d.p.}) \end{aligned} \tag{38}$$

Q4

After running the Python program on our model, let us first look at the spectra for model X and model Z, i.e. the methods of considering only the vertical or horizontal displacements of the bridge, as given by (14) and (15) respectively.

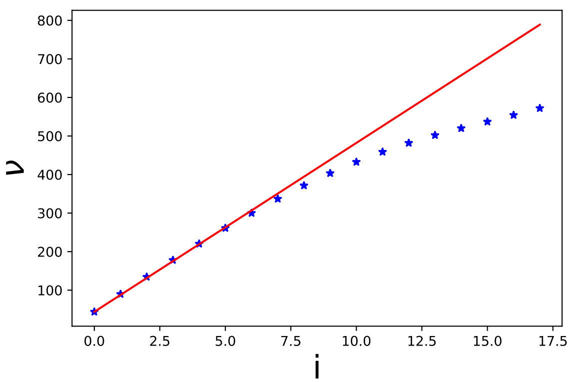

(a) Model X (Horizontal)

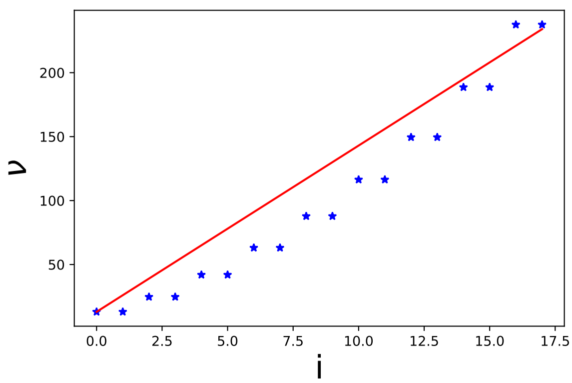

(b) Model Z (vertical)

Figure 2: Frequency spectra (frequencies against normal mode index) of model X and model Z

In the figure, the red line represents the expected harmonic frequencies of the bridge in respective dimensions extended from the lowest frequency obtained, while the blue points represent the frequencies generated by our model. We see that the blue points representing the 7 lowest frequencies of Model X matches with the red line and hence the harmonic frequencies. However, they start to divert from the red line as the frequencies get higher. On the other hand, the blue points in model Z barely match with the harmonic frequencies for the vertical displacement.

From the frequency point of view, we observe that most of the normal mode frequencies of model X are higher than model Z, where the 4 lowest modes of frequencies of model X are 43.8, 89.8, 134.4 and 178.0 Hz, while for model Z, they are 13.0, 13.0, 24.7 and 24.7 Hz. Hence, we also expect the normal frequencies which predominantly correspond to X are higher than Z when considering both vertical and horizontal displacements of the bridge. In fact, if we look at 4 higher normal mode frequencies generated by model XZ (bridge model considering both vertical and horizontal displacements): 50.3, 96.9, 143.5, 189.2 Hz, we will also observe that the 4 lowest frequencies of model X come close to them, but not approximately the same. While no frequency in model Z comes close to the 17 lower frequencies in model XZ which range from 0.8 to 5.7 Hz. Note that the lowest frequency in model Z starts at 13.0 Hz.

Let us also look at the 4 lowest mode profiles of model X and Z.

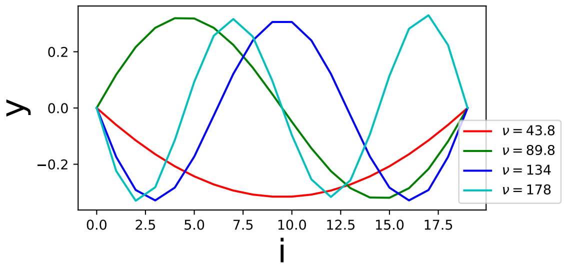

(a) Model X

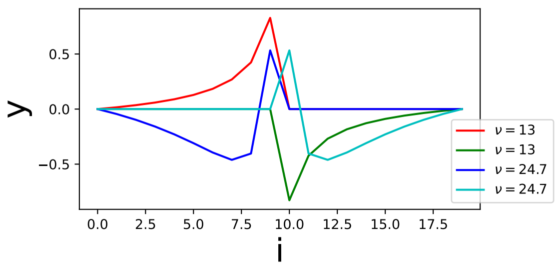

(b) Model Z

Figure 3: 4 lowest modes of model X and model Z considering only the vertical or horizontal displacements (relative amplitude against node index)

We observe that in model X, the 4 lowest modes show sinusoidal curves with 0.5 period, 1 period, 1.5 periods and 2 periods respectively, satisfying our observation of the solutions in harmonic frequencies. But for model Z, the 4 lowest profiles generated have irregular shapes. We may want to compare them with the 4 lowest normal mode profiles of model XZ:

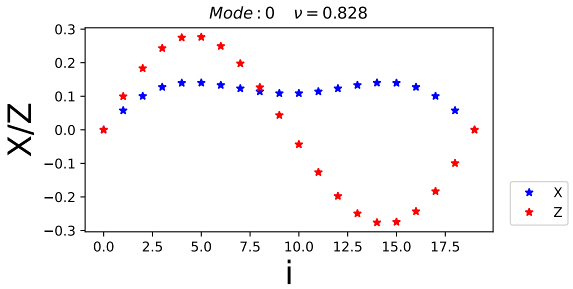

(a) Mode 0

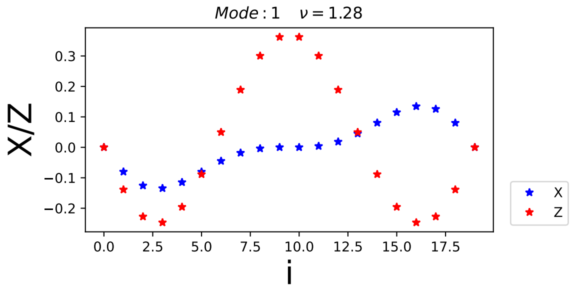

(b) Mode 1

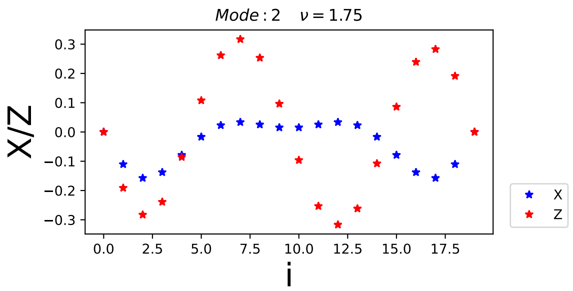

(c) Mode 2

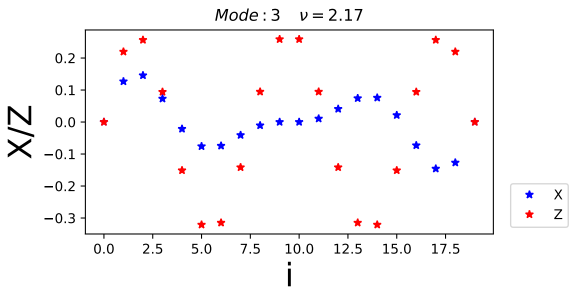

(d) Mode 3

Figure 4: 4 lowest modes of the profiles of model XZ considering both vertical and horizontal displacements (relative amplitudes against node index)

By comparing the profiles, we however realize that the waveforms in model X and model Z do not match with their respective waveforms in model XZ for the first 4 modes. In fact, we realize the waveforms of the first 4 modes in model X show similarity to the waveforms in mode 18 to 21 of model XZ. This is because the natural frequencies of model X are higher than model Z as we anticipated earlier. On the other hand, the waveforms in model Z do not match with any profiles generated by model XZ.

Hence, we can deduce that for a certain range of normal frequencies (43+ Hz), model X is a reasonably good approximation for the horizontal displacement of the bridge, but we cannot explain the other waveform patterns of the horizontal displacements at other frequencies (e.g. below 43Hz) corresponding to model XZ from the approximation. Model Z is not a good approximation either, for both lower or higher frequencies. Therefore, to consider the full set of normal modes, we should not use the two approximations.

5 A coupled oscillating system

Having looked at the three model profiles, we may also want to know about some further implications of the profiles of model XZ at different modes.

As we see in the 4 lowest profiles in figure (4), in terms of structure, the profile for vertical displacement has a more sinusoidal shape while horizontal displacement has a more irregular shape. This is because the normal frequencies of Z are lower than X, and hence at lower frequencies, normal mode frequencies for vertical displacements of the bridge are attained, giving it a more sinusoidal shape than for horizontal displacement in the profiles.

In terms of amplitude, the relative amplitudes of horizontal displacement is about $\frac{1}{2}$ or $\frac{1}{3}$ of vertical displacement. Hence, they are still comparable in relative amplitudes.

Now, let us look at the profiles of higher modes :

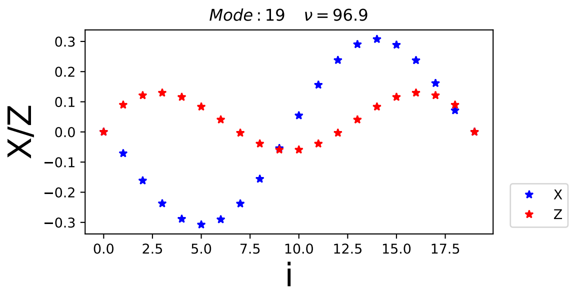

(a) Mode 19

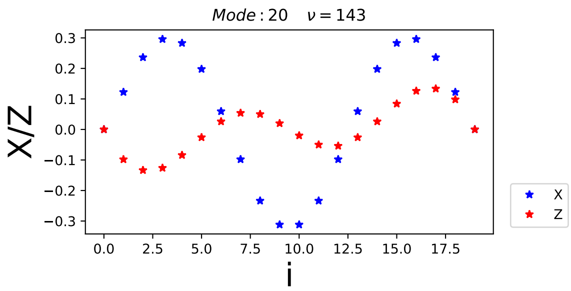

(b) Mode 20

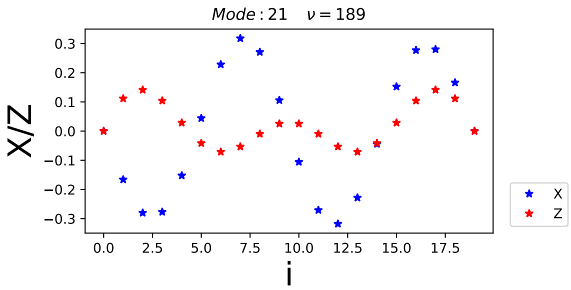

(c) Mode 21

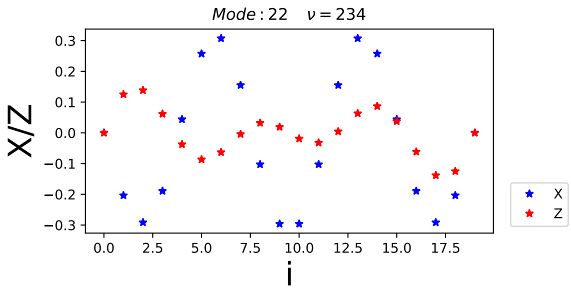

(d) Mode 22

Figure 5: 4 higher modes of the profiles of model XZ considering both vertical and horizontal displacements (relative amplitudes against node index)

As expected, in terms of structure, we see that horizontal displacement has a more sinusoidal shape than vertical displacements at higher frequencies.
In terms of amplitude, the relative amplitude of vertical displacement is about $\frac{1}{3}$ of that of horizontal displacement. They are comparable in amplitudes. Hence, it matches with our expectation that they exhibit a coupled oscillating system.

6 The full dynamic equations

Having investigated in the normal mode profiles of our coupled oscillating system, We now want to consider the full set of dynamic equations. Note that we have calculated the normal modes of the full set of the dynamic equations from our Python program, we would then like to solve them. Consider the following equations:

$$
\begin{aligned}
M\frac{d^2X_i}{dt^2} &= F_{x,i} - \Gamma\frac{dX_i}{dt} \\
M\frac{d^2Z_i}{dt^2} &= F_{z,i} + \Gamma K_{bend}\left(\frac{Z_{i-1}+Z_{i+1}}{2} - Z_i\right) - \Gamma\frac{dZ_i}{dt}
\end{aligned} \tag{39}
$$

for $i \in [1, N-1)$ where the gamma terms are added to model friction of the bridge. We can also rewrite the equations as follows, as a system of $4(N-2)$ first order differential equations: **Q6**

$$
\begin{aligned}
\frac{dx_i}{dt} &= v_{x_i} \\
\frac{dz_i}{dt} &= v_{z_i} \\
M\frac{dv_{x_i}}{dt} &= F_{x,i} - \Gamma v_{x_i} \\
M\frac{dv_{z_i}}{dt} &= F_{z,i} + K_{bend}\left(\frac{Z_{i-1}+Z_{i+1}}{2} - Z_i\right) - \Gamma v_{z_i}
\end{aligned} \tag{40}
$$

From equations (39), (13) and (12), the full dynamic equations for the bridge are shown as follows:

$$
\begin{aligned}
M\frac{d^2Z_i}{dt^2} &= K_{sc}[(X_{i-1}-X_i)\sin(\theta_i)\cos(\theta_i) + (X_{i+1}-X_i)\sin(\theta_{i+1}) + \cos(\theta_{i+1}) \\
&\quad +(Z_{i-1}-Z_i)\sin^2(\theta_i) + (Z_{i+1}-Z_i)\sin^2(\theta_{i+1})] \\
&\quad +K_{bend}\left(\frac{Z_{i-1}+Z_{i+1}}{2} - Z_i\right) - \Gamma\frac{dZ_i}{dt}
\end{aligned} \tag{41}
$$

$$
\begin{aligned}
M\frac{d^2X_i}{dt^2} &= K_{sc}[(Z_{i-1}-Z_i)\sin(\theta_i)\cos(\theta_i) + (Z_{i+1}-Z_i)\sin(\theta_{i+1}) + \cos(\theta_{i+1}) \\
&\quad +(X_{i-1}-X_i)\cos^2(\theta_i) + (X_{i+1}-X_i)\cos^2(\theta_{i+1})] - \Gamma\frac{dX_i}{dt}
\end{aligned} \tag{42}
$$

7 Load attachment simulation

After expressing the full dynamics equations of our bridge in the desired form, we are now interested to design a model to know the effect of a load on the oscillations of our bridge.

Since we are modelling a pedestrian bridge, we want to simulate a person jumping on our bridge at different positions, and at different frequencies, in order to test the effect on the amplitudes of oscillations of our pedestrian bridge. We let *pos* be the index position of the segment on which a person jumps, where the force on the central section of the deck is of the form : **Q7**

$$W = -800H(sin(2\pi vt)) \tag{43}$$

where $H(x) = x$ if $x > 0$ and $H(x) = 0$ otherwise.

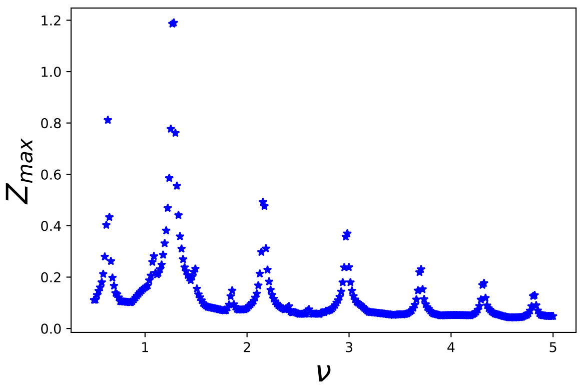

(a) pos=10

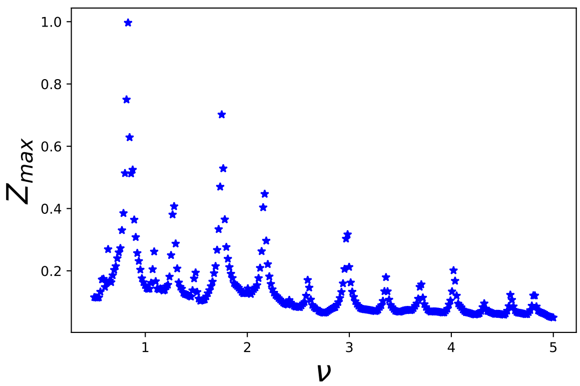

(b) pos=7

Figure 6: Plots showing the maximum vertical displacement against different frequencies

As we see in the figure above, we test for Z_{max} for 300 equal spaced points between $v = 0.5$ to $v = 5$.

Resonance occurs when frequency of the load matches with the normal mode frequency. As we compare the frequencies in figure (a) and (b) such that the amplitude of Z_{max} is at an higher level compared to the neighbouring, we indeed observe that they are generated at frequencies that matches approximately with the normal mode frequencies. It implies that during resonance, we expect to have a much larger oscillation, to a dangerous level that could break the structure of the bridge.

We could represent our observations in the following frequency table (in Hz):

Normal mode frequencies	Z_{max} frequencies (pos=10)	Z_{max} frequencies (pos=7)
0.828	0.635	0.831
1.276	1.283	1.283
1.752	1.855	1.749
2.167	2.156	2.156
2.594	No obvious peak	2.592
2.977	2.968	2.968
3.358	No obvious peak	3.360
3.700	3.706	3.706
4.027	No obvious peak	4.022
4.316	4.323	4.323
4.582	No obvious peak	4.579
4.813	4.804	4.804

As we can see in the table, the frequencies where the vertical displacement maximizes are very close to the normal mode frequencies of the bridge, implying that resonance has happened there. This accounts for the collapse of a bridge due to wind excitation. When it happens to resonate with the bridge's normal mode, it will as well oscillate in a dangerously large amplitude, causing the collapse of the bridge in the worst scenario.

As for the difference in position of the load leading to different amplitudes of Z_{max}, we have a higher maximum amplitude for $pos = 10$ than $pos = 7$. This is because when we apply the load at the middle of the bridge, it is physically intuitive that the perturbation matches the sinusoidal wave with our initial boundary condition, producing a 'perfect sine wave', thus giving us a larger amplitude than in any other position. However, the frequencies that the Z_{max} peaks at are also close to the normal frequencies of the bridge.

Besides, interestingly, we also notice that placing the load at different positions, like $pos = 7$, can potentially trigger more peaks of Z_{max} at certain normal mode frequencies that does not peak for $pos = 10$.

8 Model implications

8.1 Bridge engineering implications

From an engineering point of view, resonance is a dangerous phenomenon to structures of the bridge. It can damage its structural integrity seriously and cause destruction without any sign. Therefore, when engineers design the suspension bridge, one must consider any cause of resonance, limiting its resonating amplitude, or changing the normal mode frequency of the bridge such that they do not match with any possible cause of collapse, such as wind and earthquake.

Nowadays, improvements in the construction of suspension bridges has been made. More suspension bridges are aerodynamically streamlined, or stiffened against torsional motion. Some bridges are also equipped with shock absorbers. Wind tunnel testing for aerodynamic effects on bridges is also commonplace. [3]

Q8

8.2 Variations of bridge properties in the model

When we modelled the curved deck bridge, we have not considered some variations of properties of the bridge that could have affected the oscillations.

In terms of energy loss, the damping properties have not been studied in our model. However, damping may reduce oscillation amplitudes of the bridge over time, It may also change the natural frequency of the bridge, potentially reducing resonance of the bridge with the winds. Therefore, it crucially impacts the bridge oscillations over time in our model.

In terms of material properties, we have not considered the stiffness of the bridge. As more pedestrians use the bridge, cracks may form on the surface and its stiffness may reduce over time, and potentially make the bridge crack or collapse. In addition, the thermal expansion and density properties of the bridge has not been included in our model. Changes in environmental temperature could cause these properties to vary.

In terms of the load , we have only studied the simulation of one person jumping up and down at two different positions. However, we have not considered the effect of more than one person on the bridge, which may produce different oscillation properties.

However, due to the complexity in studying these properties, we have not included them in our current bridge model.

8.3 Application of the model to flat deck bridges

Our model could be applicable on flat deck bridges if we make some modifications. There are few differences from our bridge model. Firstly, since the deck segments have the same length, the length of the suspension cable sections varies in the flat deck bridge. Secondly, for flat deck bridges, the deck segments lie below instead of above the suspension cable, connected by the vertical suspenders. To modify our model, we would need to consider different lengths of deck segments, and separate the deck segments and vertical suspenders into two distinct but coupled oscillating systems, which is complicated to model but applicable.

9 Conclusions

In this essay, we studied a suspension bridge model to investigate its oscillations. We started with deriving the dynamic equations of a bridge and approximated it by two models considering the vertical and horizontal displacements respectively. We applied various mathematical computation techniques like Taylor expansion and eigenvalues to rewrite the equations and solve them. Then we also considered the full set of equations considering both dimensions and ran a Python program to generate profiles for analysis. We then deduced that we should consider the full model instead of the approximations. We also showed that the bridge model approximates a coupled oscillating system depending on both vertical and horizontal displacements.

Next, we considered the simulation of a person jumping on the bridge at different frequencies and positions and obtained interesting results in the model. We noticed way higher amplitudes at frequencies that match with the normal mode frequencies, indicating resonance, and there are more resonance frequencies occurring for $pos = 7$ than $pos = 10$, but a higher maximum amplitude at $pos = 10$ than $pos = 7$.

Finally, we made some model implications, including the engineering prospects on avoiding resonance and other factors that lead to collapse, and concluded some variations of other bridge properties not considered in our model, as well as the application of our model to flat deck bridges.

References

[1] The Tacoma Bridge collapse: https://www.youtube.com/watch?v=j-zczJXSxnw

[2] Weiwei Lin, Teruhiko Yoda, *Bridge Engineering*, 2017 https://www.sciencedirect.com/topics/engineering/suspension-bridges

[3] Improvements in suspension bridge construction technique: https://wsdot.wa.gov/tnbhistory/bridges-failure.htm